Disruption of Allosteric Response as a Mechanism of Resistance to Antibiotics in Staphylococcus aureus

Jennifer Fishovitz[1], Alzoray Rojas-Altuve[2], Lisandro H. Otero[2], Matthew Dawley[1], Cesar Carrasco-López[2], Mayland Chang[1], Juan A. Hermoso[2], and Shahriar Mobashery[1]

[1]Department of Chemistry and Biochemistry, Nieuwland Science Hall, Notre Dame, Indiana 46556, United States. [2]Department of Crystallography and Structural Biology, Inst. Química-Física "Rocasolano", CSIC, Serrano 119, 28006 Madrid, Spain.

The first three authors contributed equally to this work.

Email: mobashery@nd.edu and xjuan@iqfr.csic.es

Supporting Information

Contents

Experimental Procedures

Cloning, expression, and purification of PBP2a mutants. Wild-type PBP2a (residues 23-668) was cloned previously into pET24d(+) from the *mecA* sequence of *Staphylococcus aureus* ATCC 700699 (1). Mutants of *mecA* were cloned by PCR using the following mutagenic primers:

Mutation	Primer	Sequence
N146K	for	5'-GCAAACATATTGAAAAGTTAAAATCAGAACTGG-3'
	rev	5'-CCACGTTCTGATTTTAACTTTTCAATATGTATGC-3'
E150K	for	5'-CATATTGAAAATTTAAAATCAAAACGTGGTGGTAAAATTTTAGACCG-3'
	rev	5'-CGGTCTAAAATTTTACCACGTTTTGATTTTAAATTTTCAATATG-3'
N146K/ E150K	for	5'-GCATACATATTGAAAAGTTAAAATCAAAACGTGG-3'
	rev	5'-CCACGTTTTGATTTTAACTTTTCAATATGTATGC-3'
H351N	for	5'-CTCAGGTACTGCTATCAACCCTCAAACAGGTG-3'
	rev	5'-CACCTGTTTGAGGGTTGATAGCAGTACCTGAG-3'

The triple mutant (N146K/E150K and H351N) was the final product of successive PCR mutagenesis. The presence of the desired mutations was confirmed by DNA sequencing. Wild-type and mutant proteins were expressed and purified as previously described[1] with some variations. PBP2a containing fractions from anion-exchange chromatography were combined and purified on a cation-exchange column (High S support resin, Bio-Rad) using a 0.2 – 1 M NaCl linear gradient in 25 mM HEPES (pH 7). Fractions containing PBP2a were pooled and further purified on Sephacryl S-200 size-exclusion resin in 25 mM HEPES (pH 7), 1 M NaCl. Pure PBP2a was quantified by the BCA assay (Pierce).

Determination of Kinetic Parameters.

β-Lactam antibiotics acylate PBP2a at the active-site serine resulting in an acyl-enzyme species, as shown in Scheme S1.

$$E + \mathrm{I} \underset{}{\overset{K_s}{\rightleftharpoons}} E\mathrm{I} \xrightarrow{k_2} E\text{-}\mathrm{I} \qquad \text{Scheme S1}$$

where *E* is wild-type or mutant PBP2a, *E*I is the non-covalent pre-acylation complex, and *E*-I is the covalent acyl-enzyme species.

The second-order rate constant (k_2/K_s) for acylation of PBP2a by nitrocefin was determined as previously described.[1,2] For ceftaroline acylation of wild-type and mutant PBP2a the k_2/K_s value was determined by a competition assay using nitrocefin as a reporter.[2,3] Nitrocefin (120 μM) and enzyme (2.5 μM) concentrations were kept constant and the formation of the acyl-enzyme species

(E-I) was monitored at 500 nm ($\Delta\varepsilon_{500}$ = 15900 $M^{-1}cm^{-1}$) over time at 37 °C in the absence and presence of varying amounts of ceftaroline (0-12 μM). No measurable acylation by nitrocefin was observed at concentrations above 10 μM ceftaroline for wild-type PBP2a. The time course of A_{500} was fit to equation S1,[3]

$$A = A_0 + \Delta\varepsilon_n E_0(k_n^*/(k_n^* + k_i^*)(1 - \exp(-(k_n^* + k_i^*)t)) + k_0 N_0 \Delta\varepsilon_n E_0 t \qquad \text{Equation S1}$$

where A is absorbance at 500 nm, A_0 is initial absorbance at 500 nm, $\Delta\varepsilon_n$ is the change in molar absorbance of nitrocefin upon formation of the acyl-enzyme species (15,900 $M^{-1}cm^{-1}$), E_0 is the concentration of PBP2a (2.5 μM), k_n^* is the apparent first-order rate constant for acylation by nitrocefin, k_i^* is the apparent first-order rate constant for acylation by ceftaroline, and N_0 is the concentration of nitrocefin used (60 μM). The second-order rate constant k_2/K_s was determined by linear regression of k_i^* vs concentration of ceftaroline (Figure S1 and Table 1 in the manuscript).

Determination of Allosteric Site Binding Affinity by Fluorescent Quenching.

In order to investigate the binding of β-lactam antibiotics to the allosteric site of PBP2a, the transpeptidase active site of wild-type and mutant PBP2a was irreversibly acylated by incubation with an excess amount of oxacillin for 45 minutes at room temperature. Unbound oxacillin was removed with a protein desalting column (Pierce) and the acylated protein was used in subsequent experiments. Binding of ceftaroline to the allosteric site was determined by monitoring the intrinsic fluorescence of tryptophan and tyrosine residues of wild-type and mutant PBP2a. Using a Cary Eclipse fluorometer, 500 nM PBP2a was incubated at room temperature in buffer containing 25 mM HEPES pH 7, 1 M NaCl for 10 minutes. Upon excitation at 280 nm, emission scans of protein alone were taken, one scan per minute for three minutes. Ceftaroline or nitrocefin was titrated into the reaction 1 μL at a time and at each concentration three emission scans were taken (one per minute). The decrease in fluorescent emission at 330 nm for each concentration of ceftaroline was quantified and the decrease in fluorescence due to dilution was subtracted (determined by titration of buffer). The normalized difference in fluorescence was plotted versus antibiotic concentration. All experiments were done at least in triplicate and the averaged data was fit with the one-site binding equation S2,

$$Y = \frac{B_{max} * [AB]}{K_d + [AB]} \qquad \text{Equation S2}$$

where B_{max} is the maximal binding, [AB] is the concentration of ceftaroline or nitrocefin titrated, and K_d is the dissociation constant.

Crystallization.

The PBP2a single mutants (E150K, N146K) and the double mutant (N146K/E150K) were crystallized by the sitting-drop vapor diffusion method at 4 ºC using Innovaplate™ SD-2 microplates as previously described.[2] The protein solution (1 μL from each mutant concentrated up to 15–20 mg/ml) was mixed with 0.5 μL of precipitant solution consisting of 20% (v/v) PEG 550 MME, 880 mM NaCl and 16 mM $CdCl_2$ in 100 mM Hepes pH 7.0. The drop (approximately 1.5 μL of protein and precipitant solutions) was equilibrated against 50 μL of mother liquor.

X-ray data collection and processing.

Prior to flash-cooling at 100K, crystals were soaked in a 70:30 (v/v) mixture of paratone/paraffin oil for cryo-protection. Diffraction data sets were collected using synchrotron radiation (beamlines ID29, ID23-1) at the ESRF facility (France), (beamline XALOC) ALBA (Spain). An in-house equipment (MicroStart rotating anode generator and a MAR345 detector) was also used to collect data sets and to test crystals. All diffraction data sets were processed using iMOSFLM[4] or XDS[5] and scaled with SCALA from the CCP4 package[6]. Data collection statistics are shown in Table 2 in the manuscript.

Structure determination and refinement.

Structures were solved by molecular replacement using the PHASER program[7] with the PBP2a structure from *S. aureus* (PDB code 1VQQ) as template. The models were subjected to several refinement cycles with the PHENIX[8] and BUSTER[9] programs. Water molecules were added with both programs. The stereochemistry of the models was verified with the MolProbity program[10]. Refinement statistics are given in Table 2 in the manuscript.

Table S1. New salt-bridge interactions (*) observed in the clinical PBP2a mutants.
Residues are colored according to their structural regions (Lobe-1 in blue, Lobe-2 in black, Lobe-3 in red).

N146K/E150K Mutant		
	Lys146···Asp295	3.8Å
	Lys148···Asp295	2.9Å
	Lys150···Glu239	3.4Å
	Asp275···Lys273	4.8Å
	Glu294···Lys319	3.6Å
	Glu294··· Lys316	2.7Å
	Glu268··· Lys285	3.0Å
	Glu263··· Lys280	2.6Å
	Lys219···Asp367	3.7Å
	#Glu378··· Lys382	14.1Å
	#Asp209··· Lys176	5.7Å
	#Asp226··· Lys230	11.2Å
N146K Mutant		
	Lys148···Glu239	3.4Å
	Glu268···Lys285	3.6Å

* Only salt-bridge interactions not present in the wild-type PBP2a enzyme (PDB code 1VQQ) are listed.
# These salt-bridges are observed in the wild-type PBP2a enzyme but not in the clinical mutant (distances found in the clinical mutant are indicated) .

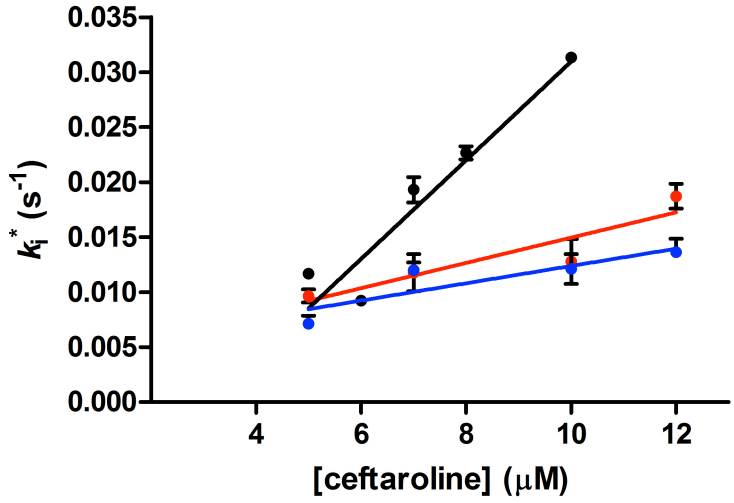

Figure S1. The second-order rate constant k_2/K_s for acylation of PBP2a by ceftaroline is derived from the linear regression of the observed rate of acylation (k_i^*, Equation S1) of wild-type (black), N146K/E150K (blue), and N146K/E150K/H351N (red) versus ceftaroline concentration.

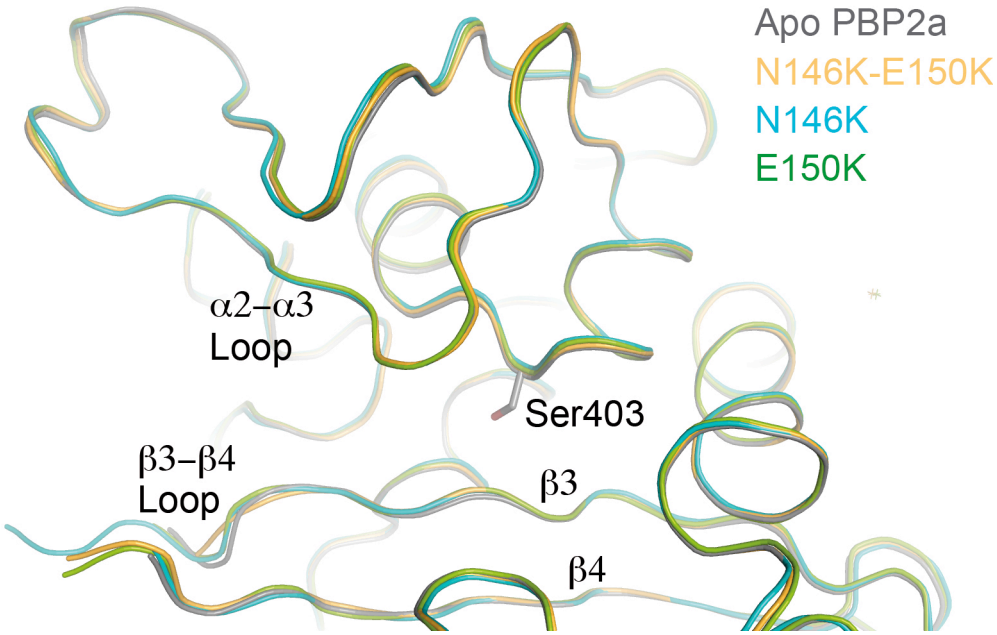

Figure S2. Structural superimposition in the active sites among apo PBP2a and the E150K, N146K and N146K-E150K variants of PBP2a. Apo PBP2a (gray ribbons), the N146K-E150K mutant (yellow ribbons), the N146K mutant (blue ribbons) and the E150K mutant (green ribbons) present an essentially identical closed conformation for their active sites (catalytic Ser403 is represented in sticks and labeled). The two important active-site loops (β3-β4 and α2- α3) are labeled.

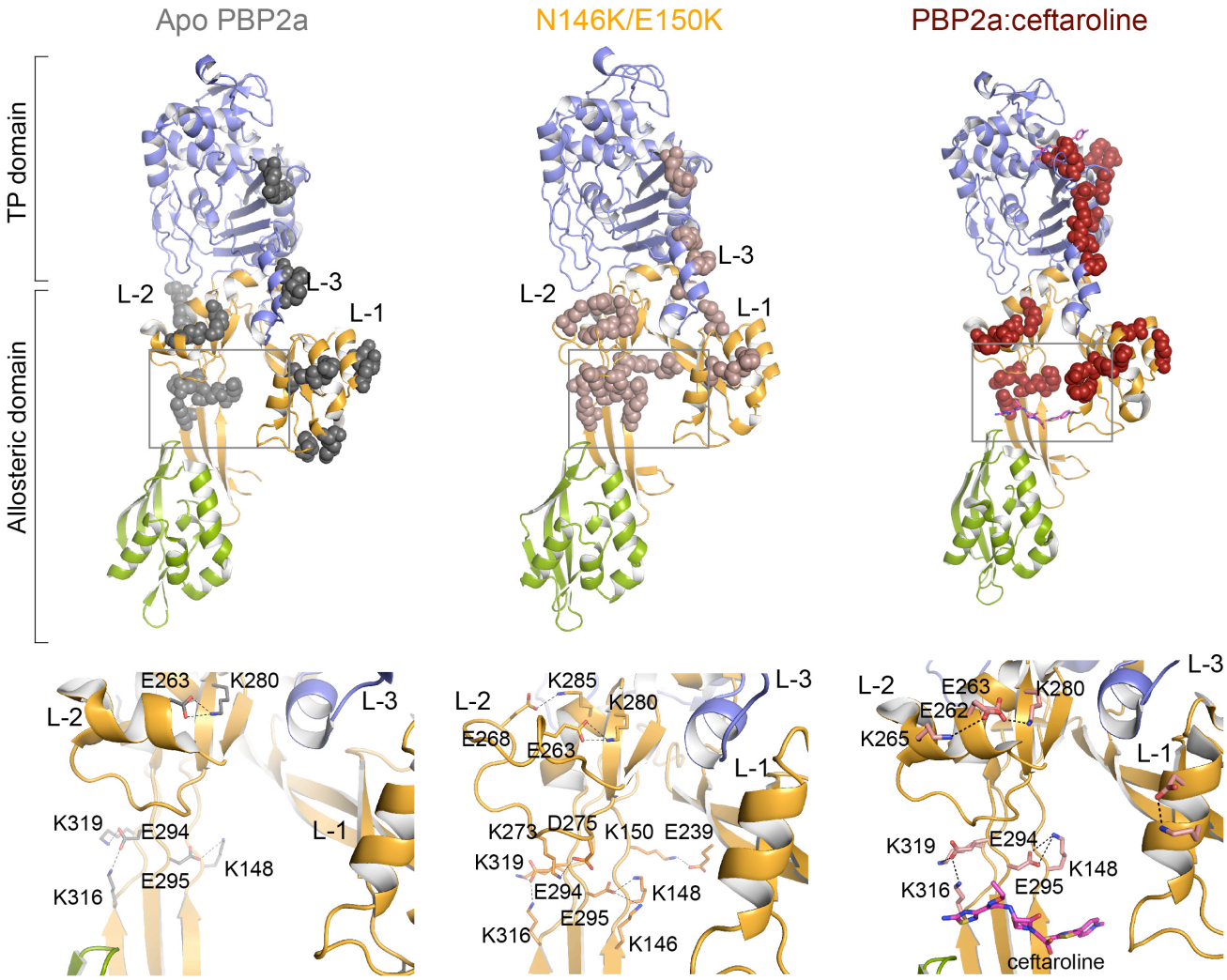

Figure S3. Comparison between the salt-bridges connecting the allosteric site with the catalytic site in the apo PBP2a (PDB code 1VQQ), the clinical N146K-E150K PBP2a mutant and the PBP2a:ceftaroline complex (PDB code 3ZG0). The N-terminal extension is colored in green, the remaining allosteric domain in yellow and the transpeptidase domain in blue. Lobes 1 (L-1), 2 (L-2) and 3 (L-3) of the allosteric site are labeled. Side-chains of residues involved in these salt-bridge interactions are represented as spheres colored in grey (apo PBP2a), in brown (N146K-E150K mutant) or in red (PBP2a:ceftaroline complex). A detailed view of the differences for the salt-bridge network in the boxed area is also represented for each protein. Ceftaroline molecules (within the active site and the allosteric site) are represented in pink sticks for the carbon atoms. The mutations in the core of the allosteric site in the double-mutant PBP2a alter the network.

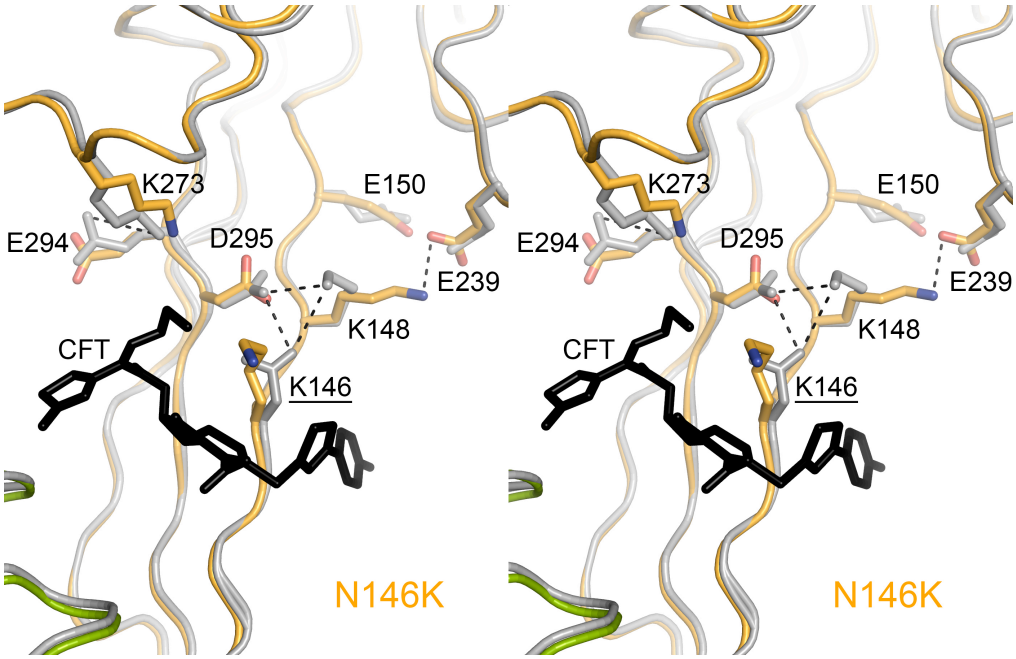

Figure S4. Stereo view of the superimposition between apo PBP2a and PBP2a single mutant N146K. Apo PBP2a (gray ribbons) and the N146K mutant (ribbons colored by domains, allosteric in gold and green and TP in blue) showed a different polar interactions (dashed lines) pattern at the allosteric site. The ceftaroline (CFT) bound at the allosteric site as observed in PDB code 3ZFZ is superimposed and depicted in black sticks. Residues involved in polar interactions are shown as grey and yellow sticks for apo PBP2a and the N146K single mutant respectively. The interactions N146···K148···D295 and K273···E294 observed in apo PBP2a, are not found in the N146K mutant. Instead, is this structure, K148 interacts with E239 (from Lobe-1).

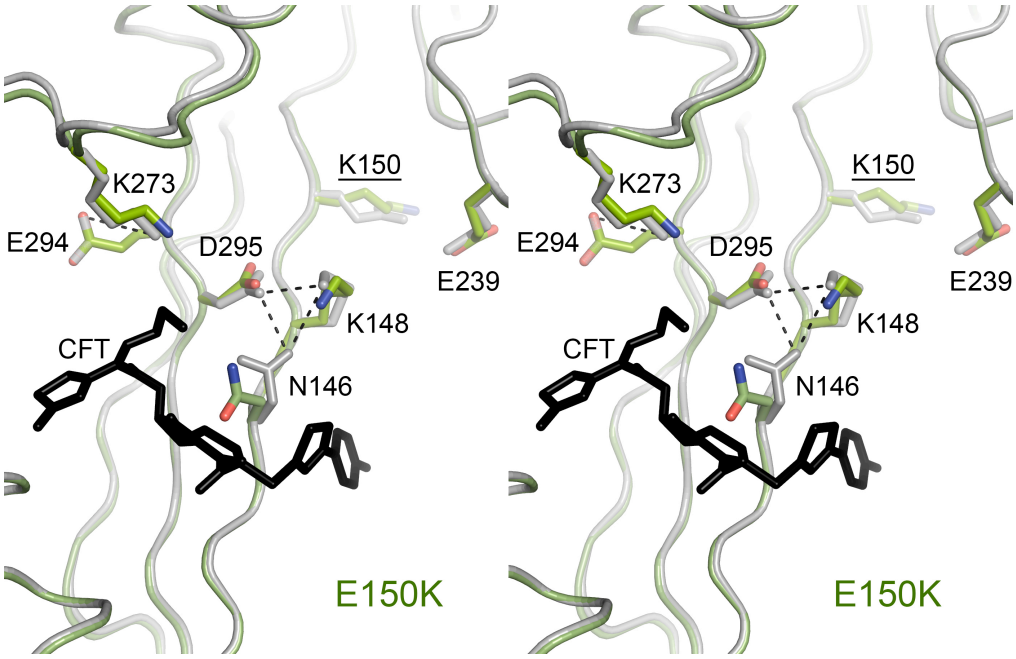

Figure S5. Stereo view of the superimposition between apo PBP2a and PBP2a single mutant E150K. Apo PBP2a (gray ribbons) and the E150K mutant (green ribbons) showed a similar polar interactions pattern at the allosteric site. The ceftaroline (CFT) bound at the allosteric site as observed in PDB code 3ZFZ is superimposed and depicted in black sticks. Residues involved in polar interactions are shown as grey and green sticks for apo PBP2a and the E150 single mutant respectively. In the E150K mutant the N146 is not participating in the interaction N146···K148···D295 observed in apo PBP2a, nonetheless the other two residues have the same conformation and interact in a salt bridge between them (K148···D295).

References

1. Fuda, C., Suvorov, M., Vakulenko, S. B., Mobashery, S. The basis for resistance to beta-lactam antibiotics by penicillin-binding protein 2a of methicillin-resistant *Staphylococcus aureus*. *J. Biol. Chem.* **2004**, 279,40802–40806.

2. Otero, L. H.; Rojas-Altuve, A.; Llarrull, L. I.; Carrasco-Lopez, C.; Kumarasiri, M.; Lastochkin, E.; Fishovitz, J.; Dawley, M.; Hesek, D.; Lee, M.; Johnson, J. W.; Fisher, J. F.; Chang, M.; Mobashery, S.; Hermoso, J. A. How allosteric control of *Staphylococcus aureus* penicillin binding protein 2a enables methicillin resistance and physiological function. *Proc. Natl. Acad. Sci. U.S.A* **2013**, 110, 16808-16813.

3. Graves-Woodward K., Pratt R. F. Reaction of soluble penicillin-binding protein 2a of methicillin-resistant *Staphylococcus aureus* with beta-lactams and acyclic substrates: kinetics in homogeneous solution. *Biochem. J.* **1998**, 332, 755-761.

4. Battye, T., Kontogiannis, L., Johnson, O., Powell, H., Leslie, A. iMOSFLM: a new graphical interface for diffraction-image processing with MOSFLM. *Acta Crystallogr. Sect. D: Biol. Crystallogr.* **2011,** 67, 271-281.

5. Kabsch, W. XDS. *Acta Crystallogr. Sect. D: Biol. Crystallogr.***2010**, 66, 125-132.

6. Collaborative Computational Project, Number 4. The CCP4 suite: Programs for protein crystallography. *Acta Crystallogr. Sect. D: Biol. Crystallogr.***1994**, 50, 760–763.

7. McCoy, A., Grosse-Kunstleve, R., Adams, P., Storini, L., Read, R. Phaser crystallographic software. *J. Appl. Cryst.* **2007***,* 40, 658–674.

8. Adams, P. D. et al. PHENIX: A comprehensive Python-based system for macro-molecular structure solution. *Acta Crystallogr. Sect. D: Biol. Crystallogr.***2010**, 66, 213-221.

9. Bricogne, G., Blanc, E., Brandl, M., Flensburg, C., Keller, P., Paciorek, W., Roversi, P., Sharff, A., Smart, O.S., Vonrhein, C., Womack, T.O. *BUSTER version X.Y.Z.* **2011,** Cambridge, United Kingdom: Global Phasing Ltd.

10. Chen, V., Arendall, W. B., Headd, J., Keedy, D. A., Immormino, R. ., Kapral, G. J., Murray, L. W., Richardson, J. S., Richardson, D. C. MolProbity: All-atom structure validation for macromolecular crystallography. *Acta Crystallogr. Sect. D: Biol.Crystallogr.***2010**, 66, 12–21.